Journal of Power Sources 194 (2009) 397–407

Contents lists available at ScienceDirect

Journal of Power Sources

journal homepage: www.elsevier.com/locate/jpowsour

A model-based parametric analysis of a direct ethanol polymer electrolyte membrane fuel cell performance

G.M. Andreadis, A.K.M. Podias, P.E. Tsiakaras*

Department of Mechanical and Industrial Engineering, School of Engineering, University of Thessaly, Pedion Areos, 383 34, Volos, Greece

ARTICLE INFO

Article history:
Received 19 December 2008
Received in revised form 10 March 2009
Accepted 26 April 2009
Available online 3 May 2009

Keywords:
Direct ethanol PEM fuel cell
Mathematical model
Parametric analysis
Ethanol crossover
Parasitic current formation
Fuel cell polarization performance

ABSTRACT

In the present work, a model-based parametric analysis of the performance of a direct ethanol polymer electrolyte membrane fuel cell (DE-PEMFC) is conducted with the purpose to investigate the effect of several parameters on the cell's operation. The analysis is based on a previously validated one-dimensional mathematical model that describes the operation of a DE-PEMFC in steady state. More precisely, the effect of several operational and structural parameters on (i) the ethanol crossover rate from the anode to the cathode side of the cell, (ii) the parasitic current generation (mixed potential formation) and (iii) the total cell performance is investigated. According to the model predictions it was found that the increase of the ethanol feed concentration leads to higher ethanol crossover rates, higher parasitic currents and higher mixed potential values resulting in the decrease of the cell's power density. However there is an optimum ethanol feed concentration (approximately 1.0 mol L^{-1}) for which the cell power density reaches its highest value. The platinum (Pt) loading of the anode and the cathode catalytic layers affects strongly the cell performance. Higher values of Pt loading of the catalytic layers increase the specific reaction surface area resulting in higher cell power densities. An increase of the anode catalyst loading compared to an equal one of the cathode catalyst loading has greater impact on the cell's power density. Another interesting finding is that increasing the diffusion layers' porosity up to a certain extent, improves the cell power density despite the fact that the parasitic current increases. This is explained by the fact that the reactants' concentrations over the catalysts are increased, leading to lower activation overpotential values, which are the main source of the total cell overpotentials. Moreover, the use of a thicker membrane leads to lower ethanol crossover rate, lower parasitic current and lower mixed potential values in comparison to the use of a thinner one. Finally, according to the model predictions when the cell operates at low current densities the use of a thick membrane is necessary to reduce the negative effect of the ethanol crossover. However, in the case where the cell operates at higher current densities (lower ethanol crossover rates) a thinner membrane reduces the ohmic overpotential leading to higher power density values.

1. Introduction

Direct Ethanol PEM Fuel Cells (DE-PEMFCs) attract the increasing interest of many researchers, due to the advantages of the feed fuel, which is hydrogen rich, less toxic and has higher energy density compared to the widely used alcohol in these devices, methanol. Moreover, ethanol as a liquid fuel can be stored, handled and distributed more easily than hydrogen and it is considered renewable, since it can be obtained mainly from the fermentation of biomass. However, the use of ethanol in PEM fuel cells is accompanied with a series of challenges that have to be overcome. The main drawbacks of DE-PEMFCs that limit their application as competitive devices are (i) the slow kinetics of the ethanol electro-oxidation reaction over the anode electrocatalyst, (ii) the fact that the electro-oxidation of ethanol below 100 °C does not proceed all the way to carbon dioxide, but rather to acetaldehyde and acetic acid indicating that the problem of the C–C bond cleavage cannot be sufficiently resolved by the up-to-date tested electrocatalysts and (iii) the ethanol crossover from the anode to the cathode side of the cell leading to the parasitic oxidation reaction of ethanol on the cathode electrocatalyst, hindering the oxygen reduction reaction (ORR). The above mentioned problems have been the subject of several experimental works dealing with DE-PEMFCs [1–17].

The performance of DE-PEMFCs depends on numerous parameters, such as the ethanol feed concentration, the operating temperature, the specific area of the catalyst where the ethanol electro-oxidation and the ORR take place, the design parameters of the different layers comprising the fuel cell, the resistance of the catalyst layer, the conductivity of the membrane, the rate of the

* Corresponding author. Tel.: +30 24210 74065; fax: +30 24210 74050.
E-mail addresses: geandrea@uth.gr (G.M. Andreadis), andreaskmp@hotmail.com (A.K.M. Podias), tsiak@mie.uth.gr (P.E. Tsiakaras).

0378-7753/$ – see front matter © 2009 Published by Elsevier B.V.
doi:10.1016/j.jpowsour.2009.04.064

Nomenclature

A_v	specific reaction surface area
$A_v i^{EtOH}_{o,ref}$	anode reference exchange current density times area
$A_v i^{O_2}_{o,ref}$	cathode reference exchange current density times area
A_s	catalyst surface area per unit mass of catalyst
$C_{F,EtOH}$	ethanol feed concentration (mol L^{-1})
C^{ref}_{EtOH}	reference ethanol concentration (mol L^{-1})
C_{F,O_2}	oxygen feed concentration (mol cm^{-3})
$C^{ref}_{O_2}$	reference oxygen concentration (mol cm^{-3})
E^{Nernst}	Nernst potential
F	Faraday's constant (96,484 C mol^{-1})
I	cell current density (A cm^{-2})
I_p	parasitic current density (A cm^{-2})
i	protonic current density (A cm^{-2})
m_{cat}	catalyst mass loading per unit area of the electrode
P	cell power density (mW cm^{-2})
R	universal gas constant (8.314 J mol^{-1} K^{-1})
T	cell operating temperature (K)
V	cell voltage (V)
z	number of released electrons

Greek symbols

α_a	anode transfer coefficient
α_c	cathode transfer coefficient
γ_a	order of anode reaction
γ_c	order of cathode reaction
ε^d	diffusion layer porosity
ε^c	catalyst layer porosity
η_a	anode activation overpotential (V)
η_c	cathode activation overpotential (V)
η_{ohmic}	ohmic overpotential (V)
$\eta_{crossover}$	overpotential due to the ethanol crossover (V)
$\eta_{conc,an}$	anode concentration overpotential (V)
$\eta_{conc,cath}$	cathode concentration overpotential (V)

ethanol crossover, the released products of the electro-oxidation along with their influence on the species transport and so on. However, the investigation of the impact of each of the above mentioned parameters experimentally is cost prohibitive. As a consequence, theoretical investigations are also essential for an in-depth understanding and optimization of the operation of a DE-PEMFC [18–23], and the analysis of the operating parameters that affect the cell performance is required for the further development of these devices.

In the present work, a model-based parametric analysis of the fuel cell operation is performed in order to investigate the effect of (i) the ethanol feed concentration, (ii) the Pt loading of the anode and cathode catalytic layers, (iii) the specific reaction surface area of the catalytic layers, (iv) the thickness of the Nafion membrane and (v) the porosity and thickness of the anode and the cathode gas diffusion layers and catalysts layers on (i) the ethanol crossover rate, (ii) the parasitic current generation (mixed potential formation) and (iii) the total cell performance.

2. Theory

The mathematical model development is based on our previous work [19]; as a consequence, only a brief description of the theoretical part is given here. During the mathematical model development the following assumptions were made: (a) the equations are defined in one direction (through-plane direction—cf. Fig. 1), (b) the cell operates under steady-state, isothermal conditions, (c) the model considers neither a two-phase flow regime nor a phase change taking place during operation, (d) the oxygen permeation through the polymeric membrane is negligible, and (e) from the crossovered quantity of ethanol, which is electro-oxidized over the cathode catalyst, the number of the released electrons is the same as those released over the anode catalyst. Additionally, taking into consideration the detailed reaction mechanism for the ethanol electro-oxidation over Pt based binary electrocatalysts, the product's analysis and the released electrons during a DE-PEMFC operation, the main products of the electro-oxidation reaction are acetic acid, acetaldehyde and carbon dioxide, whereas approximately three up to four electrons are released [4,11,16,19,24–26]. In the present study, it is assumed that four electrons are released during the ethanol electro-oxidation process over the anode catalyst. The dominant mechanisms concerning the fluxes of the aqueous ethanol solution as well as the humidified oxygen through the diffusion and the catalyst layers are diffusion and electro-osmosis. The ethanol transport through the PEM is the result of three phenomena: electro-osmosis, diffusion and hydraulic permeation. However, based on the assumption that at both anode and cathode compartments the pressure is equal, the term for the ethanol transport due to the hydraulic permeation is neglected in the present investigation. A schematic representation of a single DE-PEMFC together with the operational principles is depicted in Fig. 1.

The electrochemical equations used for the description of the ethanol electro-oxidation reaction and the ORR in the mathematical model are the following [19]:

$$\frac{di}{dz} = A_v i^{EtOH}_{o,ref}\left(\frac{C_{EtOH}}{C^{ref}_{EtOH}}\right)^{\gamma_a} \exp\left(\frac{z_a a_a F \eta_a}{RT}\right) \quad (1)$$

$$I + I_p = A_v i^{O_2}_{o,ref}\left(\frac{C_{O_2}}{C^{ref}_{O_2}}\right)^{\gamma_c} \exp\left(\frac{z_c a_c F \eta_c}{RT}\right) \quad (2)$$

where i is the local protonic current density; $A_v i^{EtOH}_{o,ref}$, $A_v i^{O_2}_{o,ref}$ the anode and cathode reference exchange current density times area respectively; γ the order of reaction; z_a, z_c the number of the electrons released at the anode and the cathode respectively; C_{EtOH}, C_{O_2} the local ethanol and oxygen concentrations in the catalyst layers; α_a, α_c the anode and cathode transfer coefficients respectively; while η_a, η_c is the anode and cathode activation overpotential respectively. I_p is the parasitic current (or internal current, or leakage current) originated from the electro-oxidation reaction of the crossovered ethanol quantities at the cathode catalyst layer. The equation used for the description of the I_p is the following [19,27–29]:

$$I_p = z_a F N^{EtOH}_{cross} \quad (3)$$

It should be noted however, that the catalyst layer has a complex three-dimensional microstructure; therefore, to convert the electrocatalytic surface reaction rate (Butler-Volmer or Tafel equation) into a volumetric reaction rate, the specific reaction surface area, A_v (effective catalyst surface area per unit geometric volume of the catalyst layer) is employed incorporating the noble metal loading into the model as well. The specific reaction surface area, A_v, is given as [30]:

$$A_v = \frac{m_{cat} A_s}{l_{an,cath}} \quad (4)$$

here m_{cat} is the catalyst mass loading per unit area of the electrode, A_s is the catalyst surface area per unit mass of the catalyst, and $l_{an,cath}$ is the anode or cathode compartments' thickness. In the present investigation the values for the A_s used in the model equations are according to the ones that have been cited in the literature

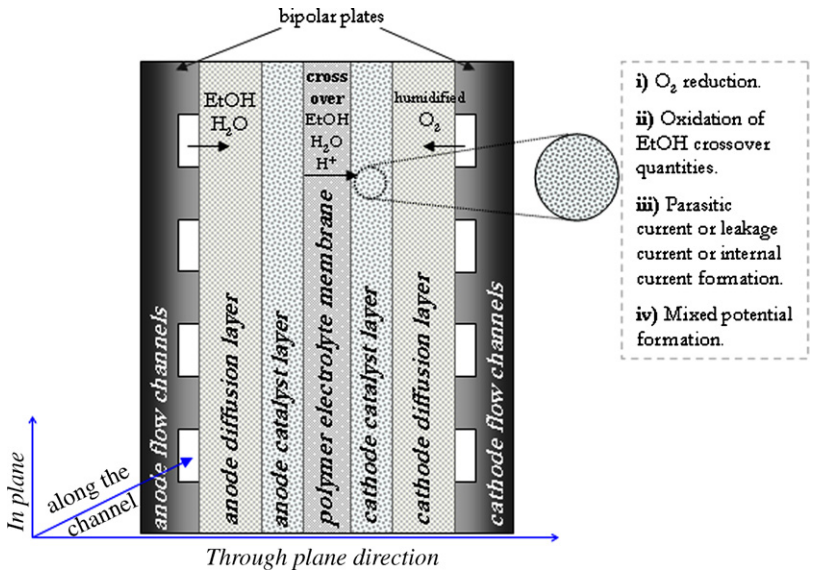

Fig. 1. Schematic representation of a DE-PEMFC and the phenomena occurring during its operation.

[30]. Finally, the total cell potential is obtained via the following equation:

$$V_{\text{cell}} = E^{\text{Nerst}} - \eta_{\text{a}} - \eta_{\text{c}} - \eta_{\text{ohmic}} - \eta_{\text{crossover}} - \eta_{\text{conc,an}} - \eta_{\text{conc,cath}} \quad (5)$$

where V_{cell} denotes the fuel cell potential; E^{Nernst} is the Nernst potential of the fuel cell at the operating temperature; η_{ohmic} the ohmic overpotential (loss in the membrane and losses between the contacts); $\eta_{\text{conc,an}}$ the anode concentration overpotential and $\eta_{\text{conc,cath}}$ the cathode concentration overpotential. The detailed equations used for the calculation of the above mentioned overpotentials are reported in our previous work [19]. For the numerical solution of the system of the governing differential equations (species mass transport balances coupled to electrochemistry) a fourth order Runge–Kutta method is implemented in an in-house FORTRAN code.

3. Results and discussion

3.1. Model validation

The mathematical model development is based on our previous work [19] and it has been validated against the experimental data presented in the literature [31]. The base case values of the parameters used in the model development are shown in Table 1.

Table 1
Base case parameter values.

Diffusion coefficient of ethanol to water, $D_{\text{EtOH}-\text{H}_2\text{O}}$ ($\text{cm}^2\,\text{s}^{-1}$)	$\frac{7.4\times10^{-8}(\Phi M_{\text{B}})^{1/2}T}{\eta_B V_{\text{A}}^{0.6}}$ [44]
Diffusion coefficient of oxygen in water, $D_{\text{O}_2-\text{H}_2\text{O}}$ ($\text{cm}^2\,\text{s}^{-1}$)	$\frac{7.4\times10^{-8}(\Phi M_{\text{B}})^{1/2}T}{\eta_B V_{\text{A}}^{0.6}}$ [44]
Diffusion coefficient of ethanol in membrane, $D_{\text{EtOH}}^{\text{m,eff}}$ ($\text{cm}^2\,\text{s}^{-1}$)	$D_{\text{m,ethanol}} = 2.1\times10^{-5}\exp\left[1319\left(\frac{1}{323}-\frac{1}{T}\right)\right]$ [19,45]
Anode diffusion layer thickness, l_{an}^{d} (μm)	140 [19,46]
Cathode diffusion layer thickness, $l_{\text{cath}}^{\text{d}}$ (μm)	140 same as anode
Anode catalyst layer thickness, l_{an}^{c} (μm)	10 [18,19,33]
Cathode catalyst layer thickness, $l_{\text{cath}}^{\text{c}}$ (μm)	10 same as anode
Nafion 115 membrane thickness, l_{m} (μm)	127 [19,45]
Reference ethanol molar concentration, $C_{\text{EtOH}}^{\text{ref}}$ ($\text{mol}\,\text{L}^{-1}$)	0.5 [18,19]
Reference oxygen molar concentration, $C_{\text{O}_2}^{\text{ref}}$ ($\text{mol}\,\text{cm}^{-3}$)	$0.58\times10^{-6}(1-p_{\text{sat}}^{\text{w}})$ [47]
Protonic conductivity of ionomer, K_{m} ($\text{S}\,\text{cm}^{-1}$)	0.1416 [19,48]
Anode transfer coefficient @ 75 °C, α_{a}	0.071 [31]
Cathode transfer coefficient, α_{c}	1.0 [34,49]
Order of reaction (anode), γ_{a}	0.25 [18,19]
Order of reaction (cathode), γ_{c}	1 [19,50]
Anode catalyst loading ($\text{mg Pt}\,\text{cm}^{-2}$)	1
Anode catalyst loading ($\text{mg Pt}\,\text{cm}^{-2}$)	1
Catalyst surface area per unit mass of the catalyst A_{s} ($\text{m}^2\,\text{g}^{-1}$)	112 [30]
Anode reference exchange current density times area @ 75 °C, $A_{\text{v}}i_{\text{o,ref}}$ ($\text{A}\,\text{cm}^{-3}$)	0.1474 [30,31]
Anode reference exchange current density times area @ 50 °C, $A_{\text{v}}i_{\text{o,ref}}$ ($\text{A}\,\text{cm}^{-3}$)	0.05152 [30,31]
Cathode reference exchange current density times area @ 75 °C, $A_{\text{v}}i_{\text{o,ref}}^{\text{O}_2}$ ($\text{A}\,\text{cm}^{-3}$)	0.033044 [30,51]
Cathode reference exchange current density times area @ 50 °C, $A_{\text{v}}i_{\text{o,ref}}^{\text{O}_2}$ ($\text{A}\,\text{cm}^{-3}$)	0.0046915 [30,51]
Electronic conductivity of solid phase (PtRu/C), K_{s} ($\text{S}\,\text{cm}^{-1}$)	8.13×10^{6} [19,52]
Porosity of anode diffusion layer, ε^{d}	0.4 [19,28]
Porosity of cathode diffusion layer, ε^{d}	0.4 same as anode
Porosity of anode catalyst layer, ε^{c}	0.35 [19]
Porosity of cathode catalyst layer, ε^{c}	0.35 same as anode
Volume fraction of ionomer phase in catalyst layer, ε^{m}	0.14 [19]
Electrosmotic drag coefficient, $n_{\text{H}_2\text{O/drag}}$	3.16 [19,53,54]

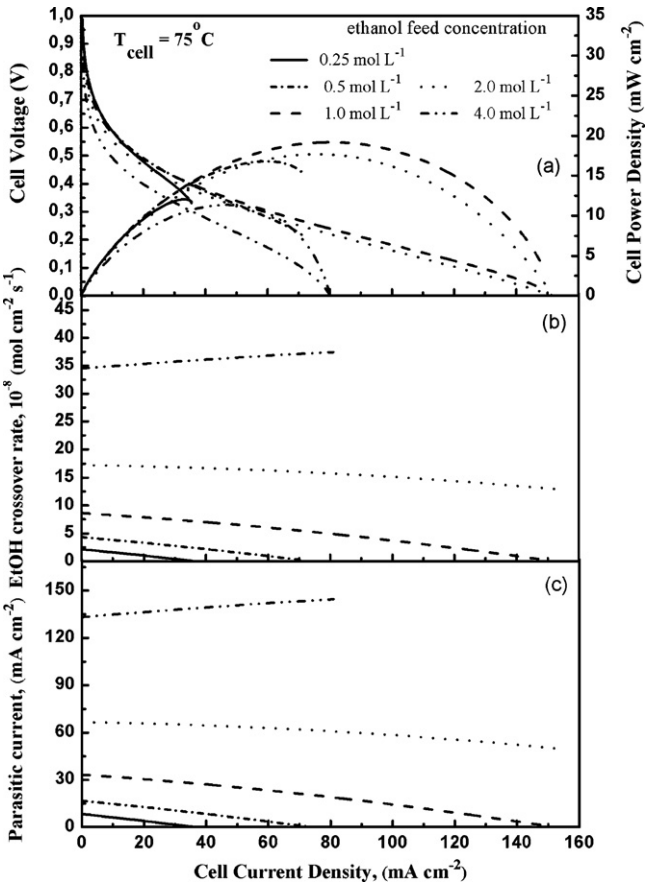

Fig. 2. Effect of ethanol feed concentration on (a) the DE-PEMFC performance, (b) the ethanol crossover rate and (c) the parasitic current formation.

3.2. Effect of ethanol feed concentration on cell performance and operation

The effect of the ethanol feed concentration on the cell performance and the parasitic current formation when the cell operates at 75 °C is depicted in Fig. 2. The Pt loading for the anode and cathode catalyst layers used in the model calculations is 1.33 mg Pt cm^{-2} and 1.0 mg Pt cm^{-2} respectively. The increase of the ethanol feed concentration from 0.25 mol L^{-1} to 1.0 mol L^{-1} improves both the cell discharge behaviour and the cell power density. However, by further increasing the ethanol feed concentration up to 4.0 mol L^{-1} the cell performance as well as the cell power density decrease. The above findings could be explained due to the fact that higher ethanol feed concentrations lead to higher ethanol crossover rates, which are directly related to higher parasitic current generation as it is shown in Fig. 2(b) and (c). The parasitic current is responsible for the mixed potential formation, which becomes higher at higher ethanol feed concentrations, deteriorating the cell performance. Moreover, the increase of the fuel feed concentration leads to lower Open Circuit Voltage (OCV) values due to the higher ethanol crossover rates.

Another point that should be noted is the effect of the cell current density on the fuel crossover rate and the parasitic current formation as well. By increasing the cell current density the ethanol crossover rate is affected in two different ways. At low ethanol feed concentrations, higher current density values result in the decrease of the fuel crossover rate, due to the fact that more ethanol molecules participate in the electrochemical reaction, thus decreasing the concentration difference between the two sides of the PEM. However, at high ethanol feed concentrations the ethanol crossover and the parasitic current increase as

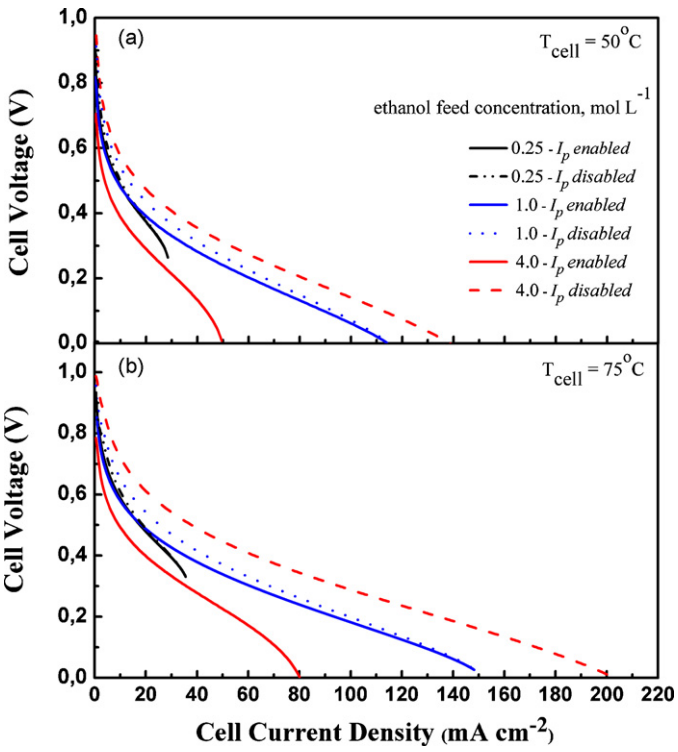

Fig. 3. The effect of the parasitic current on the DE-PEMFC performance for different ethanol feed concentrations at (a) 50 °C and (b) 75 °C.

the cell current density increases. This is explained by the fact that the ethanol crossover rate is affected by two combined transport mechanisms: (a) the diffusive transport due to the concentration differences between the anode and the cathode side of the cell and (b) the electro-osmotic drag. As the cell current density increases, the ethanol concentration difference between the anode and the cathode is reduced since more ethanol is involved in the ethanol electro-oxidation at the anode side. On the other side, the electro-osmotic drag increases due to the fact that more protons are transported through the membrane, which leads to more ethanol molecules permeated to the cathode. The resultant effect of these two phenomena could give a reasonable explanation for the observed results, which have also been reported for the case of direct methanol fuel cells [29,32–34].

The term of the parasitic current (I_p), which is directly associated with the potential losses due to the ethanol crossover and the unwanted ethanol electro-oxidation (hindering the ORR) over the cathode catalyst is necessary to describe the operation of a DE-PEMFC. In all PEM fuel cells, some current is lost due to these parasitic processes, even in the case of hydrogen PEMFCs [35–37]. The net effect of this loss is to offset the fuel cell's operating current by an amount given by the term I_p. In other words, the fuel cell has to produce extra current to compensate for the current that is lost due to the parasitic effects. Fig. 3 illustrates the effect of the parasitic current (mixed potential) when the cell is operated at two different temperatures and different ethanol feed concentrations. Solid lines depict the cell performance predictions when the parasitic current formation is enabled in the model equations (taking into account the mixed potential effect), while the dashed lines depict the cell operation when the parasitic current formation is not considered (ideal case). It is observed that among the most noticeable effects of the parasitic current formation is the reduction of the fuel cell's OCV (cf. Table 2). Additionally, the maximum cell power density is strongly affected by the existence of the I_p. It is also noted that feeding the cell with high ethanol aqueous

Table 2
OCV values at different ethanol feed concentrations and different cell temperatures (extract from Fig. 3).

$C_{F,EtOH}$ (mol L^{-1})	OCV (V) I_p *enabled*	OCV (V) I_p *disabled*
T_{cell} = 50 °C		
0.25	0.819	0.877
1.0	0.794	0.911
4.0	0.705	0.946
T_{cell} = 75 °C		
0.25	0.941	0.944
1.0	0.912	0.955
4.0	0.825	0.987

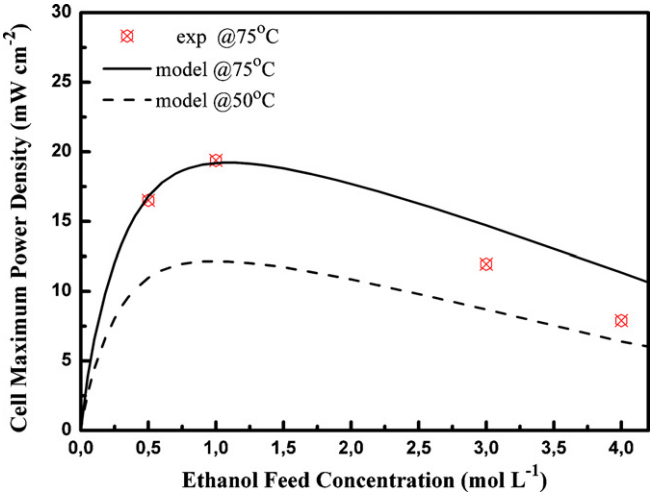

Fig. 4. The effect of the ethanol feed concentration on the maximum DE-PEMFC power density. Mathematical model predictions vs. experimental data taken from [38].

solution ($C_{F,EtOH}$ > 1.0 mol L^{-1}, i.e. 4.0 mol L^{-1}) seems to be inappropriate due to the high values of the mixed potential formation that reduces the cell power density. On the contrary, by feeding the cell with low ethanol feed concentrations ($C_{F,EtOH}$ < 1.0 mol L^{-1}, i.e. 0.25 mol L^{-1}) the negative effect of the parasitic current and the mixed potential formation is reduced. More precisely, at 75 °C the percentage of the cell power density losses due to the mixed potential formation in the case of a feed concentration of 0.25 mol L^{-1}, is approximately 0.38%, while in the case of 4.0 mol L^{-1}, the corresponding percentage is approximately 60.72%. These findings are in good agreement with the ones that have been reported experimentally in the literature and they are graphically represented in Fig. 4. A more detailed presentation of the percentages of the maximum power density losses when the cell operates at two different temperatures is shown in Table 3.

Table 3
The percentages of the losses that correspond to the cell's maximum power density values, when the effect of the parasitic current (*mixed potential*) is or is not taken into account in the mathematical model predictions.

$C_{F,EtOH}$ (mol L^{-1})	Max power density losses (%) $(P_{max}^{Ip,disabled} - P_{max}^{Ip,enabled})/P_{max}^{Ip,disabled} \times 100\%$	T_{cell} (°C)
0.25	0.465	50
1	10.1	50
4	61.65	50
0.25	0.388	75
1	8.24	75
4	60.72	75

The results correspond to the base case values for the parameters used in the model equations.

Fig. 4 shows the effect of the ethanol feed concentration on the DE-PEMFC maximum power density according to (a) the mathematical model predictions and (b) the experimental data cited in the literature (cf. Ref. [38]). The mathematical model predictions correspond to the cell operation when a PtRu/C catalyst with loading of 1.0 mg Pt cm^{-2} (20%) and a Pt/C catalyst with loading of 1.0 mg Pt cm^{-2} (20%) are used as anode and cathode catalysts respectively. From both the experimental data and the model predictions it is observed that there is an optimum ethanol feed concentration of approximately 1.0 mol L^{-1} for which the cell's maximum power density is achieved. Moreover, by increasing the feed concentration above this value, the cell performance deteriorates due to the higher ethanol crossover rates that lead to higher parasitic currents and higher mixed potential values. It is apparent from Fig. 4, that there is a good agreement between the model predictions and the experimental data for a feed concentration up to 1 mol L^{-1}. For a feed concentration above 1 mol L^{-1}, and specifically at 3 mol L^{-1}, and 4 mol L^{-1} the model over predicts the cell maximum power density. This behaviour could be attributed to the fact that at higher fuel feed concentrations the ethanol crossover rate is increased, thus, less cathode catalyst sites are available for the ORR to occur.

Fig. 5(a) and (b) shows the ethanol crossover rate as a percentage of the total ethanol flux transported from the feed stream to the anode catalyst layer (cf. Fig. 1, through-plane direction) for various current densities and feed concentrations at 50 °C and

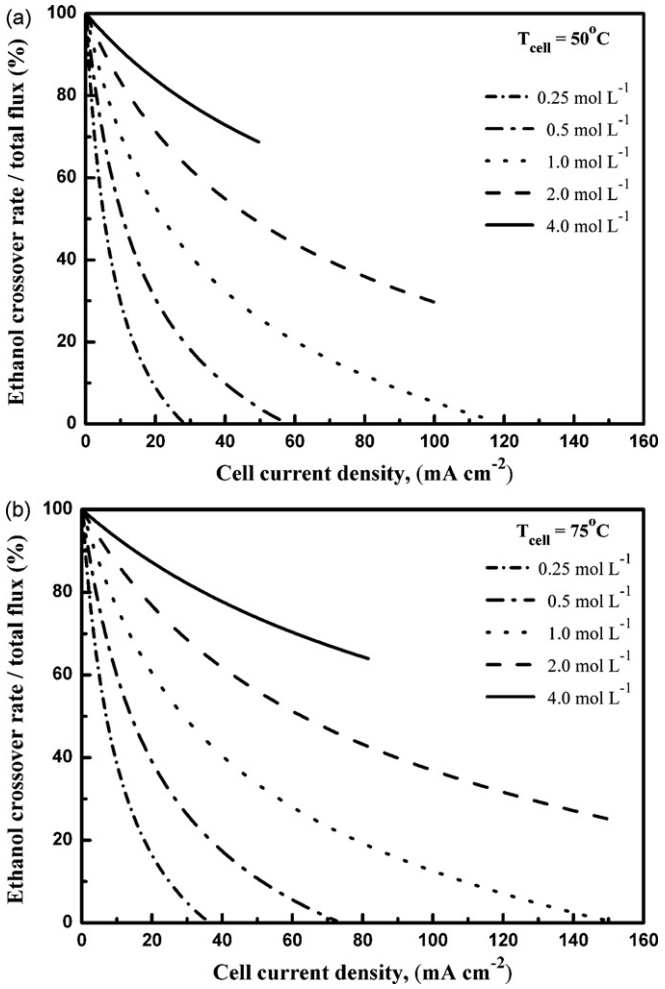

Fig. 5. The ethanol crossover rate as a percentage of the total ethanol flux vs. cell current density for various feed concentrations and different temperatures: (a) 50 °C and (b) 75 °C.

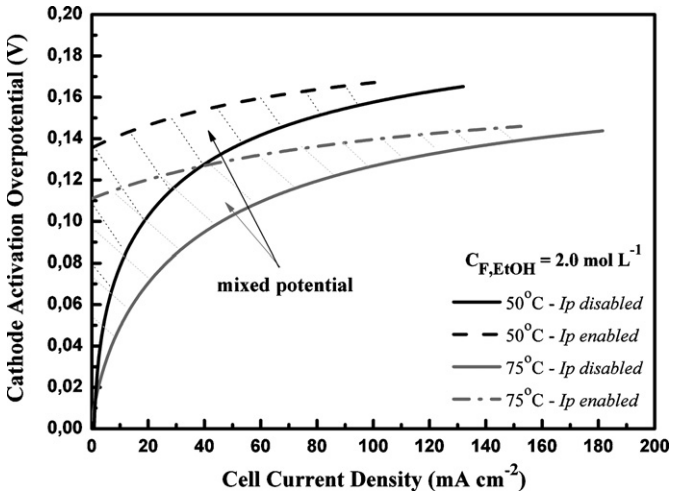

Fig. 6. Mixed potential formation in DE-PEMFC operation at 50 °C, 75 °C; ethanol feed concentration 2.0 mol L^{-1}.

75 °C. As physically expected, at low current densities, a large portion of the ethanol fed into the fuel cell is wasted because of the crossover phenomenon. In the case of 1 mol L^{-1} ethanol feed concentration, a zero fuel crossover may be obtained when the current density reaches a limiting value of approximately 0.12 A cm^{-2} (at 50 °C) and 0.15 A cm^{-2} (at 75 °C). Similar numerical findings for low methanol feed concentrations, as far as the trend of the percentage ratio is concerned, have been reported for the case of a DMFC [33]. For higher ethanol feed concentrations, i.e. 2 mol L^{-1} and current density values lower than 0.1 A cm^{-2} and 0.15 A cm^{-2}, at 50 °C and 75 °C respectively, the crossover rate is more than 30% of the total ethanol flux reaching the anode catalyst layer. The high crossover rate observed for 2 mol L^{-1} or higher ethanol feed concentration affects strongly the limiting current density, due to the high values of the parasitic currents. The effect of the parasitic current in the model results explains why at higher alcohol feed concentrations the percentage of the ethanol crossover rate could not reach the value of 0%. The latter effect is not reported in a similar work for a DMFC (e.g. [33]) due to the fact that the term of I_p was not taken into account during the mathematical model formulation.

The effect of the operating temperature on the cathode activation overpotential when the parasitic current is enabled or not in the model predictions is presented in Fig. 6. The ethanol feed concentration is 2.0 mol L^{-1} and the Pt loading of both catalyst layers is 1.0 mg Pt cm^{-2}. It is shown that the increase of the operating temperature results in the decrease of the cathode activation overpotential due to the improved kinetics of the ORR. However, the effect of the mixed potential formation is obvious in both cases, affecting: (a) the onset value of the cathode activation overpotential, (b) the limiting current density value and consequently, and (c) the total cell performance.

3.3. Effect of anode and cathode catalyst loading on the cell performance

Fig. 7(a) and (b) illustrates the effect of the anode and the cathode catalyst layer loading respectively on the DE-PEMFC performance predictions. It should be noted that the Pt loading is enabled in the mathematical model via Eq. (4) [19,30]. An increase of the Pt loading of the catalyst (m_{cat}) leads to higher values of the specific reaction surface area (A_v) resulting in better cell performance. In the present study, the values of the Pt loading used for the parametric analysis range from 0.2 mg Pt cm^{-2} to 1.33 mg Pt cm^{-2} for

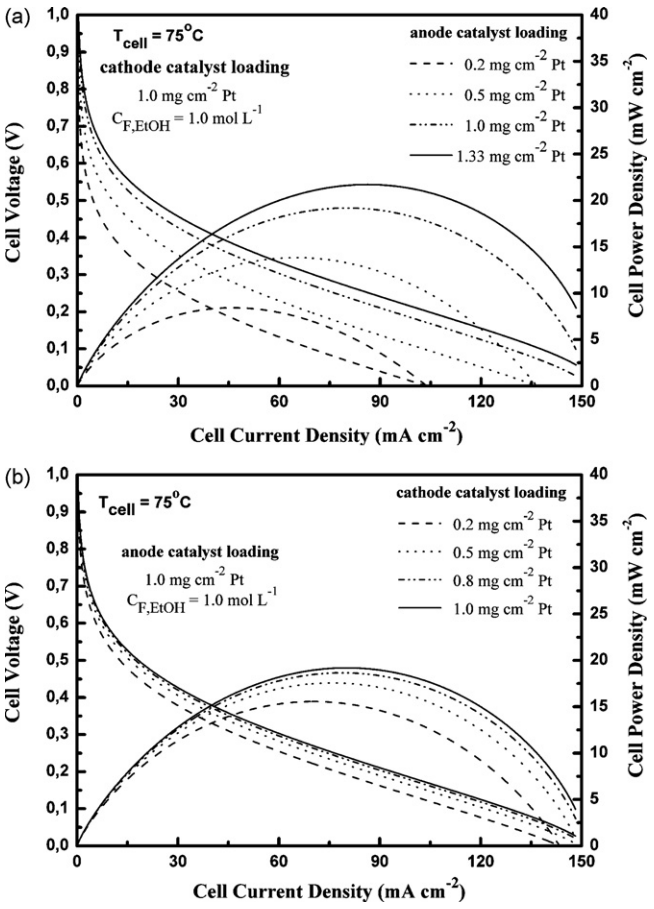

Fig. 7. Effect of (a) anode, and (b) cathode catalyst layer loading on DE-PEMFC performance.

the anode catalyst and from 0.2 mg Pt cm^{-2} to 1.0 mg Pt cm^{-2} for the cathode catalyst. For these values of the Pt loading there are many experimental data indicating the improved performance of the cell [15,31,39–41]. Generally, when the same experimental method for the catalyst preparation is followed, by increasing the Pt loading up to a certain value definitely leads to higher cell power density values. However, above a certain value of Pt loading the DE-PEMFC performance deteriorates. This is attributed to the fact that high Pt loading may not be well dispersed over the catalyst, resulting in a decrease of the catalyst layer porosity, thereby hindering the diffusion of the reactants through the electrodes [40]. According to the model predictions, the increase of the cell performance is more obvious in the case of higher anode Pt loadings than in the case of higher cathode Pt loadings. More specifically, by increasing the anode catalyst loading from 0.2 mg Pt cm^{-2} to 1.0 mg Pt cm^{-2} (see Fig. 7(a)) the cell performance is enhanced approximately by 128%. By increasing the cathode catalyst loading from 0.2 mg cm^{-2} Pt to 1.0 mg cm^{-2} Pt (see Fig. 7(b)) the cell performance is enhanced by approximately 23%. This is explained due to the fact that the ethanol electro-oxidation reaction over the anode catalyst layer is much slower than the ORR over the cathode catalyst layer. As a consequence, a higher anode specific reaction surface area has more significant effect on the cell operation compared to a higher cathode specific reaction surface area. Moreover, it could be concluded that the decrease of the Pt loading of the cathode catalyst, or the use of novel non-Pt and ethanol-tolerant electrocatalysts with approximately the same activity towards ORR could reduce the cost of a DE-PEMFC, without reducing the cell power density significantly [13,17]. On the other hand, reducing the Pt loading in the already

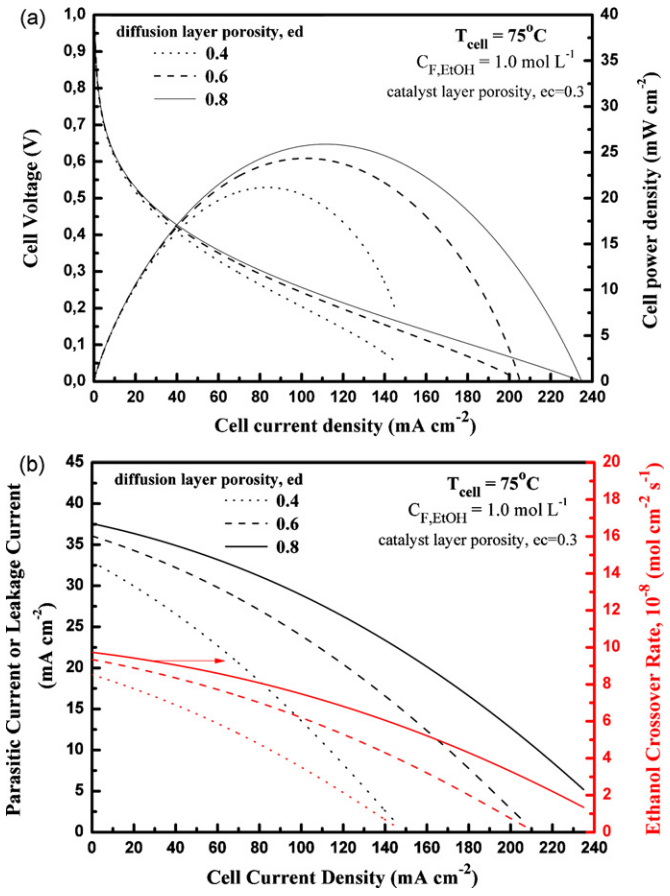

Fig. 8. The effect of the diffusion layer porosity on (a) DE-PEMFC performance and (b) ethanol crossover rate as well as the parasitic current formation.

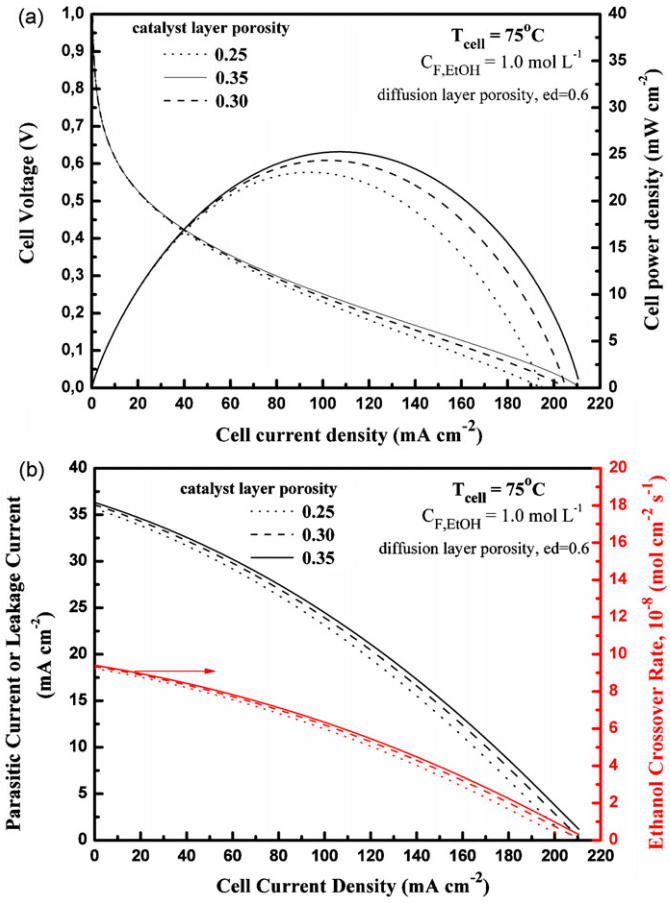

Fig. 9. The effect of the catalyst layers porosity on (a) DE-PEMFC performance and (b) ethanol crossover rate, and the parasitic current formation.

known anode electrocatalysts would definitely lead to lower cell power densities.

3.4. Effect of structural parameters on the cell operation

3.4.1. The effect of the diffusion layers' porosity on the cell performance and the formation of the parasitic current

Apart from the effect of the ethanol feed concentration on the cell performance and the mixed potential formation, it is of great importance to determine the effect of certain structural parameters on the cell operation. Thus in Fig. 8(a) and (b) the effect of the diffusion layers porosity on the DE-PEMFC performance and the parasitic current formation when the cell operates at 75 °C with 1.0 mol L^{-1} ethanol aqueous solution is presented. The Pt loading of the anode and the cathode catalyst layers is 1.33 mg Pt cm^{-2} and 1.0 mg Pt cm^{-2} respectively, while three different values of the diffusion layers porosity are examined.

As the porosity of the diffusion layers increases, the cell performance and the ethanol crossover rate (also the parasitic current) increase as well (cf. Fig. 8(b)). The higher the values of the porosity, the more ethanol and oxygen molecules reach the catalyst layers getting involved in the electrochemical reactions. As a result, the anode and the cathode activation overpotentials decrease. On the other hand, the more ethanol molecules reaching the anode catalyst layer, the higher the crossover rate and the parasitic current are. However, the combined effect of the above mentioned phenomena when the diffusion layers' porosity increases from 0.4 to 0.8 enhance the cell maximum power density approximately by 22%. A similar observation has been reported in the case of a DMFC performance as well [34].

3.4.2. The effect of the catalyst layers' porosity on the cell performance and the formation of the parasitic current

Another parameter affecting the cell performance and its operation is the porosity of the catalyst layer. The catalytic layer used in a DE-PEMFC should possess enough porosity to enable the fuel to be easily diffused and reach the catalyst active sites as effectively as possible. In Fig. 9 the effect of the catalyst layer porosity on the DE-PEMFC performance and the parasitic current formation is illustrated. The cell operates at 75 °C, the Pt loadings of the anode and cathode catalyst layers are equal to 1.33 mg Pt cm^{-2} and 1.0 mg Pt cm^{-2} respectively, and the diffusion layers porosity is equal to 0.6.

As it is shown, by increasing the catalyst layer porosity more reactants' molecules participate in the electrochemical reactions, thereby leading to slightly higher power density values. Furthermore, as the catalyst layer porosity increases, the ethanol crossover rate through the membrane and the parasitic current formation increase as well. However, it seems that this increment has smaller influence on the cell performance compared to the improved kinetics due to the higher reactants' concentrations over the catalyst layers. This behaviour could be explained due to the fact that the anode and cathode activation overpotentials are the leading source of losses during the DE-PEMFC operation [19]. To conclude, according to the mathematical model predictions, by slightly increasing the porosity of the catalyst and the diffusion layers' porosity, no matter the negative effect of the increased mixed potential on the DE-PEMFC operation, the power density increases. However, the increase of the catalyst layer porosity has minor effects on the limiting current density and the fuel crossover rates due to the fact that

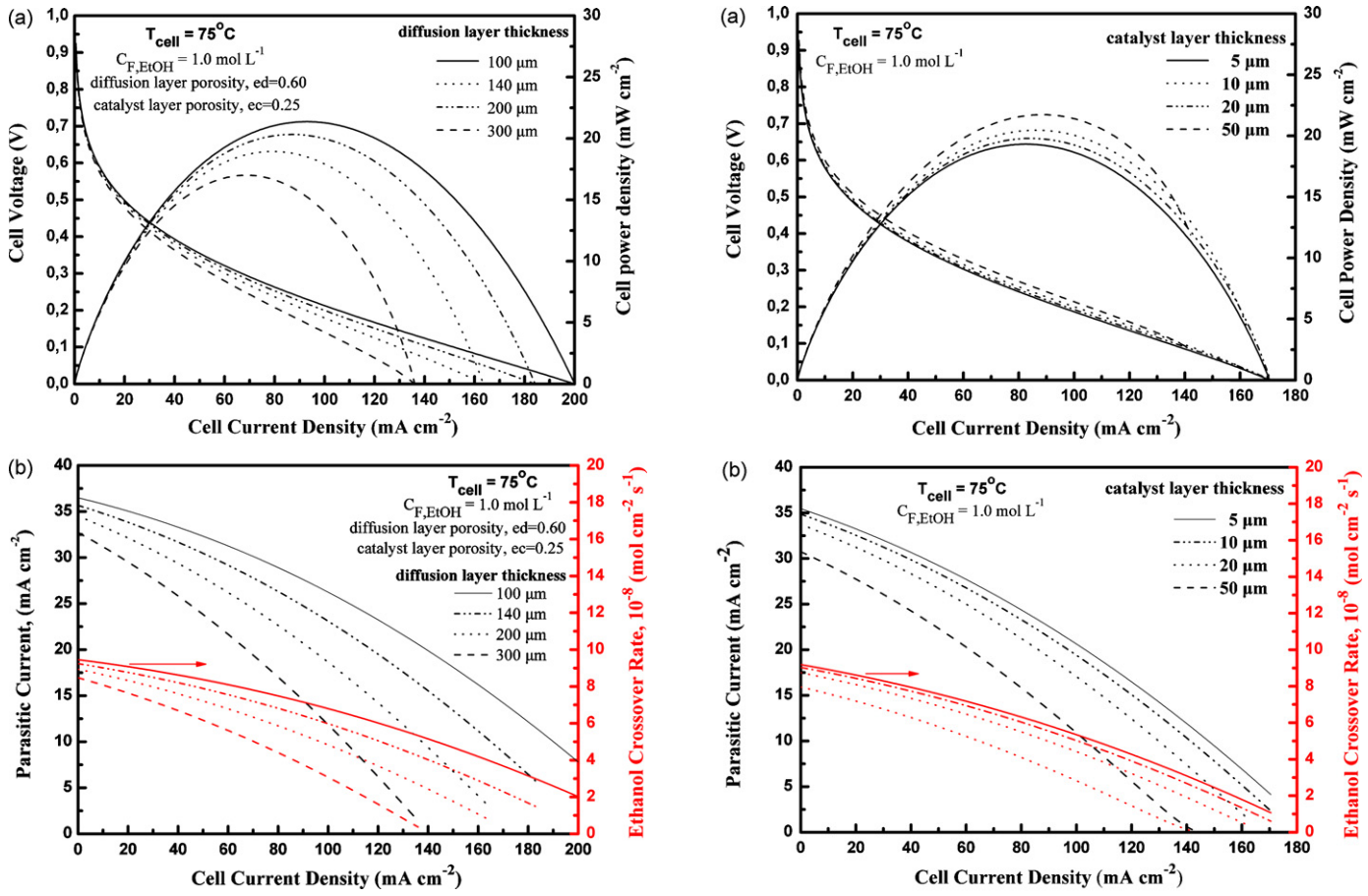

Fig. 10. The effect of the diffusion layers thickness on (a) DE-PEMFC performance and (b) ethanol crossover rate, and the parasitic current formation.

Fig. 11. The effect of the catalyst layers thickness on (a) DE-PEMFC performance, (b) ethanol crossover rate, and the parasitic current formation, and (c) spatial anode overpotential variation at constant current density.

it is much thinner than the diffusion layer and the corresponding mass transfer resistance in this layer is smaller [34].

3.4.3. The effect of the diffusion layers' thickness on the cell performance and the formation of the parasitic current

The role of the diffusion layers in DE-PEMFCs is to enhance the ethanol to water miscibility and to optimize the ethanol distribution on the catalyst layer, so for all the active sites to participate in the reaction. The effect of the diffusion layers' thickness on the DE-PEMFC performance and the ethanol crossover rate through the PEM is depicted in Fig. 10(a) and (b), where the cell operating parameters are also presented. The increase of the diffusion layers' thickness results in a decrease in the fuel cell performance. This is attributed to the fact that the limiting current density (I_{lim}) is inversely proportional to the diffusion layer thickness [19,28]. Moreover, by increasing the thickness of the diffusion layer, the quantities of the reactants reaching the anode and the cathode catalyst layers are reduced. Thus, decreasing ethanol and oxygen concentrations over the catalysts leads to increased activation overpotentials and lower cell power density values.

3.4.4. The effect of the catalyst layers' thickness on the cell performance and the formation of the parasitic current

The effect of the thickness of the catalyst layer on the DE-PEMFC performance, the ethanol crossover rate and the formation of the parasitic current is presented in Fig. 11(a) and (b). The Pt loading of the anode and cathode catalyst layers are equal to 1.0 mg Pt cm^{-2}. The porosities of the diffusion layers and the catalyst layers are equal to 0.6 and 0.3 respectively. As it is shown, by increasing the catalyst layer thickness 10 times (from 5 μm to 50 μm) the cell performance is improved approximately 12.5%. This is attributed to the fact that the thicker the catalyst layer, the more reactants could be involved in the electrochemical reactions giving rise to lower ethanol crossover rates, due to the decreased ethanol concentration difference between the two sides of the PEM, as it is depicted in Fig. 11(b). However, the use of such a catalyst implies higher internal cell resistance, which is unwanted due to the ohmic overpotentials. Thus, according to the model results, an optimum thickness of the Pt catalyst layers is approximately 10–15 μm taking into consideration both performance, as well as economical criteria.

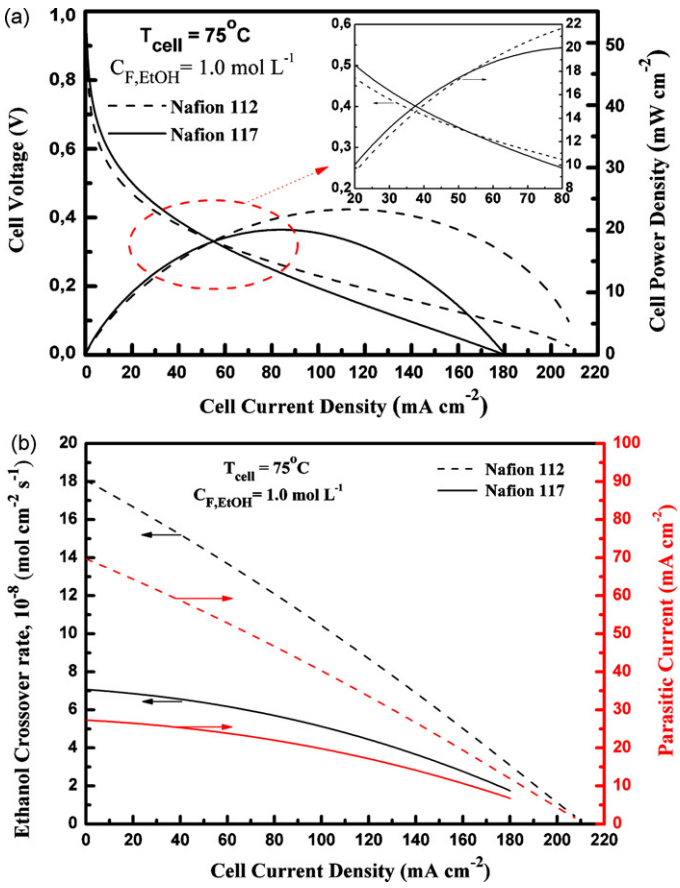

Fig. 12. The effect of the membrane used on (a) DE-PEMFC performance, and (b) ethanol crossover rate, and the parasitic current formation.

Fig. 11(c) shows the typical spatial anode activation overpotential profile over four different thicknesses of the anode catalyst layer at a constant cell current density value equal to 120 mA cm^{-2}. The overpotential increases with a parabolic profile as the catalyst layer thickness increases. Moreover, by increasing the catalyst layer thickness, this parabolic profile is more obvious, as it was also shown in the case of a DMFC [42]. A possible explanation is that a thicker catalyst layer means higher internal resistance for the ethanol to pass through, resulting in higher ohmic resistances. Additionally, it is observed that increasing the catalyst layer thickness the value of the anode overpotential is also slightly increased. This is attributed to the calculation of the specific reaction surface area, A_v parameter, which for constant Pt loading value decreases as the catalyst layer thickness increases.

3.5. Effect of the Nafion thickness on the DE-PEMFC operation

Fig. 12(a) and (b) presents the effect of the thickness of the membrane (Nafion 112 & Nafion 117) on the DE-PEMFC polarization curves, the ethanol crossover rate and the parasitic current when the cell operates at 75 °C and it is fed with 1.0 mol L^{-1} aqueous ethanol solution. As it can be seen in Fig. 12(a), the effect of the membrane thickness on the cell performance can be divided into two distinct regions. In low current densities (~50 mA cm^{-2}), the DE-PEMFC with a thicker membrane (Nafion 117) exhibits better performance, whereas in higher current densities (>50 mA cm^{-2}), the DE-PEMFC with a thinner membrane (Nafion 112) presents better performance. This finding could be explained with a closer look of Fig. 12(b). A different membrane thickness leads to a change of the ethanol crossover rate as well as the parasitic current formation. The use of a thicker membrane reduces the ethanol crossover rate due to the higher "resistance" that the fuel has to overcome to reach the cathode side of the cell, in contrast to the case of a thinner membrane. Thus, at low current densities, where the ethanol crossover rate and the parasitic current formation acquire their highest values, a thicker membrane has positive effect on the cell performance. On the one hand, due to the higher ethanol crossover rate at low current densities, a thinner membrane leads to higher values of mixed potential on the cathode, reducing the total cell performance. On the other hand, the use of a thinner membrane means smaller internal cell resistance, especially at higher current densities, leading to increased cell performance. The results of the present analysis are in accordance to what has been experimentally reported in the literature for the case of a DMFC operated with different Nafion based membranes [43]. However, the investigation of the membrane's technical specifications in DEFC performance via experiments and modelling studies is underway in our facilities and a more detailed analysis will be the subject of a future work.

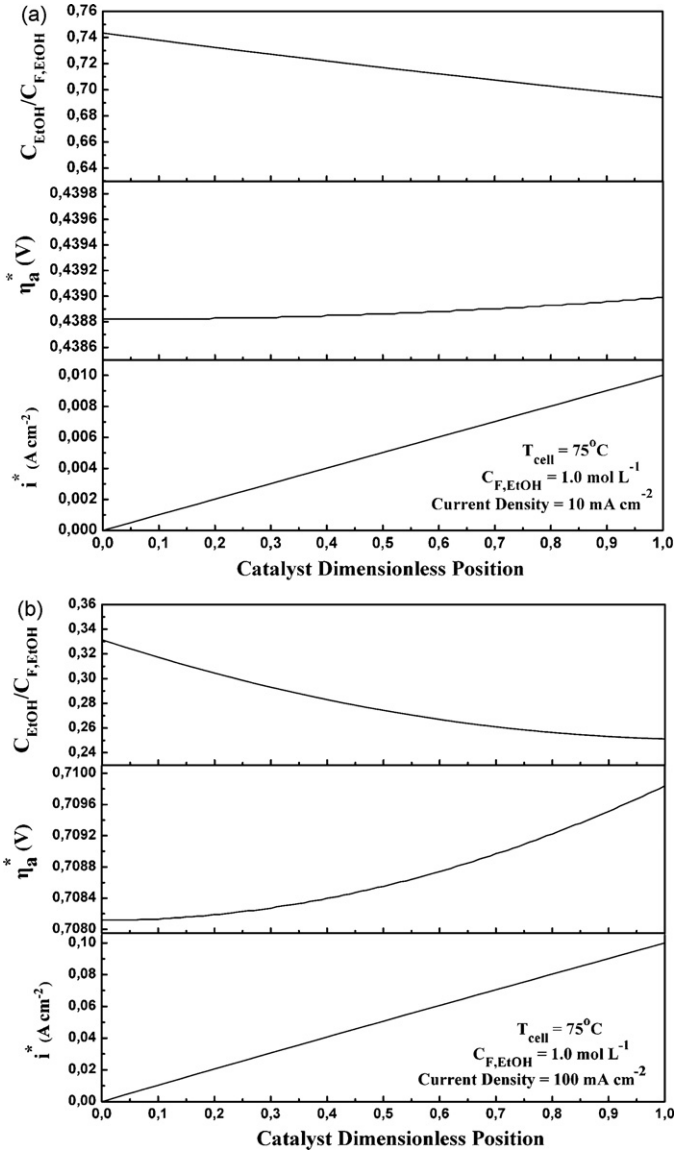

Fig. 13. Distribution of the local ethanol concentration, the local anode overpotential and the local current density across the anode catalyst layer at (a) 10 mA cm^{-2} and (b) 100 mA cm^{-2}.

3.6. Concentration, local overpotential and local current density profiles across the catalyst layer

Fig. 13(a) and (b) depicts the distribution of the ethanol concentration as a portion of the ethanol feed concentration, the local anode overpotential and the local current density across the anode catalyst layer when the cell operates at two different cell current density values (10 mA cm^{-2} and 100 mA cm^{-2}). The ethanol feed concentration is equal to 1.0 mol L^{-1} and the cell temperature equals to 75 °C. By comparing the ethanol profiles across the anode catalyst between the two cases, it is observed that at higher current densities the slope of the ethanol distribution is steeper due to the fact that more ethanol molecules should participate in the reaction in order to fulfill the requirement for high cell current density. Moreover, by examining the local overpotential distribution at small current, the local overpotential is almost constant along the catalyst layer. However, by increasing the cell current density, the overpotential distribution is not linear, and more precisely the curve shifts upward (parabolic shape along the catalyst layer thickness towards the membrane) as the dimensionless catalyst position becomes equal to one. This is a typical profile of the overpotential across the catalyst layer reported also elsewhere in the case of a DMFC [42]. Finally, the model predictions show that the local current density increases linearly along the thickness of the anode catalyst layer towards the anode catalyst layer/membrane interface.

4. Conclusions

In the present work a parametric analysis regarding the performance of a DE-PEMFC by the aid of a validated one-dimensional mathematical model was undertaken. The model predicts the fuel cell polarization performance in terms of the *V–I*, *P–I* curves, the ethanol crossover rate and the parasitic current formation for different operational and structural parameters. It was found that there is an optimum ethanol feed concentration of ~1.0 mol L^{-1} for which the cell power density obtains its highest value. Lower feed concentrations lead to lower ethanol crossover rates and lower parasitic currents, while the use of higher feed concentrations results in high ethanol crossover rates, higher parasitic currents and higher mixed potential values. The parasitic current formation hinders the fuel cell operation and its negative influences are more pronounced at higher feed concentrations, indicating the above mentioned optimum ethanol feed concentration. The most noticeable negative effects due to the mixed potential formation are (i) the substantial reduction of the fuel cell's OCV and (ii) the reduction of the fuel cell's discharge behaviour, indicating the need of more ethanol-tolerant, and/or non-Pt based electrocatalysts for the ORR. Moreover, the reduction of the anode catalyst loading has more severe effect on the cell power density in comparison to the reduction of the cathode catalyst loading by the same amount. The effect of several structural parameters was also examined. By increasing the diffusion and the catalyst layers' porosity the ethanol crossover rate and the parasitic current formation is increased. However, the negative effect of the mixed potential formation is compensated due to the fact that more reactants' molecules participate in the electrochemical reactions resulting in lower values of anode and cathode activation overpotentials. Moreover, the use of a thicker membrane leads to lower ethanol crossover rates, lower parasitic currents and lower mixed potential values in comparison to the use of a thinner one. Thus, when the cell operates at low current densities, the use of a thick membrane is necessary to reduce the negative effect of the ethanol crossover. However, in the case where the cell operates at higher current densities (lower ethanol crossover rates) a thinner membrane reduces the ohmic overpotential leading to higher power density values.

Acknowledgements

This work is part of the 03ED897 research project, implemented within the framework of the "Reinforcement Programme of Human Research Manpower" (PENED) and co-financed by National and Community Funds (25% from the Greek Ministry of Development-General Secretariat of Research and Technology and 75% from EU-European Social Fund).

References

[1] T. Lopes, E. Antolini, F. Colmati, E.R. Gonzalez, J. Power Sources 164 (2007) 111–114.
[2] C. Lamy, S. Rousseau, E. Belgsir, C. Coutanceau, J. Leger, Electrochim. Acta 49 (2004) 3901–3908.
[3] E. Antolini, J. Power Sources 170 (2007) 1–12.
[4] S. Song, P. Tsiakaras, Appl. Catal. B: Environ. 63 (2006) 187–193.
[5] E. Antolini, F. Colmati, E. Gonzalez, Electrochem. Commun. 9 (2007) 398–404.
[6] F. Colmati, E. Antolini, E. Gonzalez, Appl. Catal. B: Environ. 73 (2007) 106–115.
[7] F. Colmati, E. Antolini, E.R. Gonzalez, J. Power Sources 157 (2006) 98–103.
[8] S. Kontou, V. Stergiopoulos, S. Song, P. Tsiakaras, J. Power Sources 171 (2007) 1–7.
[9] J. Liu, J. Ye, C. Xu, S. Jiang, Y. Tong, Electrochem. Commun. 9 (2007) 2334–2339.
[10] J. Ribeiro, D.M. dos Anjos, K.B. Kokoh, C. Coutanceau, J.M. Leger, P. Olivi, A.R. de Andrade, G. Tremiliosi-Filho, Electrochim. Acta 52 (2007) 6997–7006.
[11] S. Rousseau, C. Coutanceau, C. Lamy, J. Leger, J. Power Sources 158 (2006) 18–24.
[12] S. Song, V. Maragou, P. Tsiakaras, J. Fuel Cell Sci. Technol. 4 (2007) 203–209.
[13] S. Song, Y. Wang, P. Tsiakaras, P.K. Shen, Appl. Catal. B: Environ. 78 (2008) 381–387.
[14] S. Song, W. Zhou, J. Tian, R. Cai, G. Sun, Q. Xin, S. Kontou, P. Tsiakaras, J. Power Sources 145 (2005) 266–271.
[15] P.E. Tsiakaras, J. Power Sources 171 (2007) 107–112.
[16] Q. Wang, G.Q. Sun, L. Cao, L.H. Jiang, G.X. Wang, S.L. Wang, S.H. Yang, Q. Xin, J. Power Sources 177 (2008) 142–147.
[17] T. Lopes, E. Antolini, E.R. Gonzalez, Int. J. Hydrogen Energy 33 (2008) 5563–5570.
[18] G. Andreadis, P. Tsiakaras, Chem. Eng. Sci. 61 (2006) 7497–7508.
[19] G.M. Andreadis, A.K.M. Podias, P.E. Tsiakaras, J. Power Sources 181 (2008) 214–227.
[20] R. Sousa Jr., D.M. dos Anjos, G. Tremiliosi-Filho, E.R. Gonzalez, C. Coutanceau, E. Sibert, J.-M. Leger, K.B. Kokoh, J. Power Sources 180 (2008) 283–293.
[21] I. Sarris, P. Tsiakaras, S. Song, N. Vlachos, Solid State Ionics 177 (2006) 2133–2138.
[22] A. Podias, G. Andreadis, P. Tsiakaras, Interaction of transport phenomena and electrochemistry in direct ethanol PEM fuel cells via CFD: reactants and products distribution, in: Fuel Cells Science & Technology, Scientific Advances in Fuel Cell Systems, Copenhagen, Denmark, 8–9 October, 2008.
[23] A. Podias, G. Andreadis, P. Tsiakaras, Single-phase flow and transport in a direct ethanol PEM fuel cell, in: Tenth Grove Fuel Cell Symposium, 25–27 September, London, UK, 2007.
[24] F. Delime, J. Leger, C. Lamy, J. Appl. Electrochem. 28 (1997) 27–35.
[25] H. Hitmi, E. Belgsir, J. Leger, C. Lamy, R. Lezna, Electrochim. Acta 39 (1994) 407–415.
[26] C. Lamy, A. Lima, V. LeRhun, F. Delime, C. Coutanceau, J. Leger, J. Power Sources 105 (2002) 283–296.
[27] B. Garcia, V. Sethuraman, J. Weidner, R. White, R. Dougal, J. Fuel Cell Sci. Technol. 1 (2004) 43–48.
[28] K. Yin, J. Power Sources 167 (2007) 420–429.
[29] K.M. Yin, J. Power Sources 179 (2008) 700–710.
[30] C. Marr, X. Li, J. Power Sources 77 (1999) 17–27.
[31] X. Zhao, L. Jiang, G. Sun, S. Yang, B. Yi, X. Qin, Chin. J. Catal. 25 (2004) 983–988.
[32] S. Eccarius, B.L. Garcia, C. Hebling, J.W. Weidner, J. Power Sources 179 (2008) 723–733.
[33] K. Jeng, C. Chen, J. Power Sources 112 (2002) 367–375.
[34] W. Yang, T. Zhao, Electrochim. Acta 52 (2007) 6125–6140.
[35] S.S. Kocha, J.D. Yang, J.S. Yi, AIChE J. 52 (2006) 1916–1925.
[36] J. Zhang, Y. Tang, C. Song, J. Zhang, H. Wang, J. Power Sources 163 (2006) 532–537.
[37] K. Broka, P. Ekdunge, J. Appl. Electrochem. 27 (1997) 117–124.
[38] S. Song, W. Zhou, Z. Liang, R. Cai, G. Sun, Q. Xin, V. Stergiopoulos, P. Tsiakaras, Appl. Catal. B: Environ. 55 (2005) 65–72.
[39] W. Zhou, Z. Zhou, S. Song, W. Li, G. Sun, P. Tsiakaras, Q. Xin, Appl. Catal. B: Environ. 46 (2003) 273–285.
[40] H. Pramanik, S. Basu, Can. J. Chem. Eng. 85 (2007) 781–785.
[41] H. Pramanik, A.A. Wragg, S. Basu, J. Appl. Electrochem. 38 (2008) 1321–1328.
[42] A.A. Kulikovsky, Electrochem. Commun. 7 (2005) 969–975.
[43] J.G. Liu, T.S. Zhao, Z.X. Liang, R. Chen, J. Power Sources 153 (2006) 61–67.
[44] R. Reid, J. Prausnitz, B. Poling, The Properties of Gases & Liquids, Mc-Graw Hill International Editions, Chemical Engineering Series Inc., Singapore, 1988, pp. 581–586.
[45] S. Kato, K. Nagahama, H. Asai, J. Membr. Sci. 72 (1992) 31–41.
[46] K. Scott, P. Argyropoulos, K. Sundmacher, J. Electroanal. Chem. 477 (1999) 97–110.
[47] P. Kauranen, E. Skou, J. Electroanal. Chem. 408 (1996) 189–198.
[48] K. Scott, W. Taama, J. Cruickshank, J. Power Sources 65 (1997) 159–171.

[49] C.Y. Du, T.S. Zhao, C. Xu, J. Power Sources 167 (2007) 265–271.
[50] D. Bernardi, M. Verbrugge, AIChE J. 37 (1991) 1151–1163.
[51] A. Parthasarathy, S. Srinivasan, A. Appleby, C. Martin, J. Electrochem. Soc. 139 (1992) 2530–2537.
[52] S. Baxter, V. Battaglia, R. White, J. Electrochem. Soc. 146 (1999) 437–447.
[53] X. Ren, W. Henderson, S. Gottesfeld, J. Electrochem. Soc. 144 (1997) L267–L270.
[54] T. Springer, T. Zawodzinski, S. Gottesfeld, J. Electrochem. Soc. 138 (1991) 2334–2342.